Resonance enhanced multiphoton ionisation spectroscopy of carbon disulphide

Morgan, R.A.; Baldwin, M.A.; Orr-Ewing, A.J.; Ashfold, M.N.R.; Buma, W.J.; Milan, J.B.; de Lange, C.A.

DOI
10.1063/1.471277

Publication date
1996

Published in
Journal of Chemical Physics

Resonance enhanced multiphoton ionization spectroscopy of carbon disulphide

Ross A. Morgan, Michael A. Baldwin, Andrew J. Orr-Ewing, and Michael N. R. Ashfold
School of Chemistry, University of Bristol, Bristol BS8 1TS, United Kingdom

Wybren Jan Buma, Jolanda B. Milan, and Cornelis A. de Lange
Laboratory for Physical Chemistry, University of Amsterdam, Nieuwe Achtergracht 127, 1018 WS Amsterdam, The Netherlands

(Received 27 November 1995, accepted 11 January 1996)

Rydberg excited states of the CS_2 molecule in the energy range 56 000–81 000 cm^{-1} have been further investigated via the two and three photon resonance enhancements they provide in the mass resolved multiphoton ionization (MPI) spectrum of a jet-cooled sample of the parent molecule. Spectral interpretation has been aided by parallel measurements of the kinetic energies of the photoelectrons that accompany the various MPI resonances. Thus we have been able to extend, and clarify, previous analyses of the tangled spin–orbit split vibronic structure associated with the $^3\Pi_u$ and $^1\Pi_u$ states derived from the configuration $[^2\Pi_g]4p\sigma_u$ and the $^3\Delta_u$, $^1\Delta_u$, and $^1\Sigma_u^+$ states resulting from the configuration $[^2\Pi_g]4p\pi_u$, and to deduce an approximate wave number for the origin of the hitherto unidentified $^3\Sigma_u^+$ state derived from this same configuration. Moving to higher energies we are able to locate, unambiguously, the origins of the next ($n=5$) members of four of these $[^2\Pi_g]np$ Rydberg series, and to identify extensive series based on the presumed Rydberg configurations $[^2\Pi_g]ns\sigma_g$ and $[^2\Pi_g]nf\lambda_u$ with, in both cases, $n\leqslant 10$. We also identify MPI resonances attributable to CS($a\ ^3\Pi$) fragments, to ground state C atoms, and to S atoms in both their ground (^3P) and excited (^1S) electronic states. Analysis of the former resonances indicates that the CS($a\ ^3\Pi$) fragments resulting from two photon dissociation of CS_2 at excitation wavelengths around 300 nm are formed with substantial rovibrational excitation. © *1996 American Institute of Physics.* [S0021-9606(96)00815-7]

INTRODUCTION

Both the spectroscopy[1–16] and the photochemistry[9,17–30] of excited electronic states of the carbon disulphide molecule, CS_2, have been the subject of extensive study over the past half century. Like carbon dioxide, CS_2 has a linear ($D_{\infty h}$ symmetry) ground state geometry, with 16 valence electrons arranged in the configuration

$$\cdots(5\sigma_g)^2(4\sigma_u)^2(6\sigma_g)^2(5\sigma_u)^2(2\pi_u)^4(2\pi_g)^4;\widetilde{X}\ ^1\Sigma_g^+ \qquad (1)$$

with the highest occupied $2\pi_g$ orbital being largely nonbonding in character, and with the bulk of its associated electron density located on the terminal sulphur atoms. The molecule has three fundamental modes of vibrational motion: ν_1, the symmetric stretch (which transforms as σ_g^+), ν_2, the degenerate bend (π_u) and ν_3, the asymmetric stretch (σ_u^+), the ground state frequencies of which are 658, 396, and 1535 cm^{-1}, respectively.[4]

The $\tilde{X}\ ^2\Pi_g$ ground state of the CS_2^+ ion is formed by removing an electron from the $2\pi_g$ orbital. It, too, has a linear equilibrium geometry. This ionic state is split into two spin–orbit components, of which the $^2\Pi_{g3/2}$ state is lower in energy. High resolution photoelectron spectroscopy (PES)[31–33] and, particularly, recent zero kinetic energy (ZEKE) photoelectron studies[34] have established a value of 81 286±5 cm^{-1} for this lowest ionization limit, a spin–orbit splitting of 440 cm^{-1}, and vibrational frequencies of ca. 620, 332, and 1195 cm^{-1} for, respectively, the ν_1, ν_2, and ν_3 normal modes in the ground state ion. The present study is solely concerned with Rydberg states belonging to series that converge to one or other spin–orbit component of the ground state ion.

The literature contains many reports of studies of the ultraviolet (uv) and vacuum ultraviolet (vuv) absorption spectrum of CS_2. The 290–410 nm region contains a wealth of resolved rovibronic structure, much of which has now been assigned[2,6,7,12,16] in terms of excitations to the so-called R,S,U,V, and T states—bent valence states arising as a result of the electronic promotion $3\pi_u \leftarrow 2\pi_g$. Proceeding to shorter wavelengths, the next feature of note is a reasonably intense vibronic progression spanning the region 190–210 nm; the partial analyses reported to date[3] are consistent with this being associated with excitation to the bent $^1B_2$ component of the $^1\Sigma_u^+(3\pi_u \leftarrow 2\pi_g)$ state. Price and Simpson[1] were the first to identify two Rydberg series in the vuv region, converging to the two spin–orbit components of the ground state ion.

The energy range up to and including the first ionization limit has been much studied subsequently, both in one photon absorption[1,5,8,13,14] and by electron impact spectroscopy,[10,11] but *multi*photon studies of the excited states of CS_2, have, until very recently, remained sparse. Yet, as we are reminded in Table I, it is for centrosymmetric systems like CS_2 that multiphoton studies should, potentially at least, be most valuable.[35] Indeed, the only Rydberg states for which a one photon electric dipole excitation from the

TABLE I. Orbital and upper state symmetries accessible by one, two, and three photon induced transitions from the $\cdots(2\pi_g)^4;\tilde{X}\ ^1\Sigma_g^+$ ground state. Only those upper states which can be reached on the basis of molecular selection rules are included.

Number of photons	Orbital type	Orbital symmetry	Upper state symmetry
1	p	σ_u	Π_u
		π_u	Σ_u^+
2	s	σ_g	Π_g
	d	σ_g	Π_g
		π_g	Σ_g^+,Δ_g
		δ_g	Π_g
3	p	σ_u	Π_u
		π_u	Σ_u^+,Δ_u
	f	σ_u	Π_u
		π_u	Σ_u^+,Δ_u
		δ_u	Π_u,Φ_u
		ϕ_u	Δ_u,Γ_u

ground ($\tilde{X}\ ^1\Sigma_g^+$) state should be fully allowed are those derived from the configurations involving the $^2\Pi_g$ ion core and an *ungerade* (e.g., p or f) Rydberg electron; it is generally accepted that the dominant series observed in the early absorption work[4] is associated with the $[^2\Pi_g]np\sigma_u$ configuration. Two photon excitations, in contrast, should offer the possibility of populating Rydberg states involving *gerade* Rydberg orbitals, e.g., those associated with the configurations $[^2\Pi_g]ns\sigma_g$, $[^2\Pi_g]nd\sigma_g$, $[^2\Pi_g]nd\pi_g$, and $[^2\Pi_g]nd\delta_g$, while population of additional high angular momentum Rydberg states derived from the configuration $[^2\Pi_g]nf\lambda_u$ might be anticipated in three photon excitation spectroscopy. This is the motivation behind the present study.

For completeness, we here summarize the still somewhat fragmentary conclusions of the multiphoton studies of CS_2 reported thus far. Couris *et al.*[36] have reported a 2+1 resonance enhanced multiphoton ionization (REMPI) study of the 54 000–58 000 cm^{-1} energy region and identified resonances due to the two states (derived from the two spin–orbit states of the ion core) associated with the excited configuration $[^2\Pi_g]4s\sigma_g$. Li *et al.*[37,38] and, more recently, Baker and co-workers[39,40] have investigated the energy region 62 000–65 000 cm^{-1} using both one color 3+1 and two color $(1+1')+1$ REMPI spectroscopy. As a result it is now clear that, in this energy range, the vertical electronic spectrum of CS_2 is dominated by transitions to excited states derived from the Rydberg configuration $[^2\Pi_g]4p\lambda_u$. As we show later, the present REMPI studies, supplemented by parallel measurements of the accompanying REMPI-PE spectra, serve to substantiate, and refine, many of the arguments contained in the latter works.[39,40]

Assignments proposed in a number of the earlier studies[5,8] of the Rydberg states of CS_2 have been based on analogy with the all-first-row prototype CO_2, for which a number of rotationally resolved Rydberg transitions are known and for which a limited range of *ab initio* calculations have been reported.[41] In the context of the present work it is pertinent to note that recent 3+1 REMPI and REMPI-PES studies of CO_2 have revealed the spin–orbit split $[^2\Pi_g]3p\sigma_u$ Rydberg state and a series of spin–orbit split resonances associated with the configuration $[^2\Pi_g]nf_u(n=4-13)$.[42–47] Higher members of the p Rydberg series were not observed, presumably because these excited states are heavily predissociated.[46] Excited states of the noncentrosymmetric analog OCS in the energy region 70 000–76 000 cm^{-1} have also been investigated by REMPI spectroscopy,[48–50] but because of its lower ($C_{\infty v}$) symmetry, there is no u/g parity selection rule and the parallels with CO_2 and CS_2 are expected to be less marked.

Here, we report the first comprehensive study of the entire two and three photon REMPI spectra of a jet-cooled sample of carbon disulphide up to the first ionization limit. Numerous vibronic features are apparent in each spectrum and many of these resonances can be assigned as members of well defined Rydberg series converging to the two spin–orbit components of the ground state of the molecular ion. As in the recent REMPI study of CO_2[46] definitive interpretation of the individual vibronic features appearing in these spectra has been greatly aided by concurrent measurements of the kinetic energies of the photoelectrons accompanying the REMPI process.

EXPERIMENT

The results reported here were obtained using two complementary experimental setups: In Bristol, a home-built time-of-flight (TOF) mass spectrometer was used to record *mass* resolved REMPI spectra of CS_2, and in Amsterdam REMPI-PES studies were performed using a ''magnetic bottle'' spectrometer. Both experiments have been described in detail previously[51–54] so only brief summaries of the two experimental methods are given here.

REMPI spectra were recorded using a pulsed nozzle to inject samples of CS_2 (either as a 10% mixture diluted in argon to a total pressure of ca. 1 atm, or as the pure gas) into the source region of the TOF mass spectrometer. The gas pulses were crossed by the focused (f.l.=200–300 mm) output of a tuneable Nd:YAG pumped dye laser, which was frequency doubled when necessary. Wavelength calibration of the dye laser, in the visible, was performed simultaneously with recording of REMPI spectra by measurement of the optogalvanic spectrum of neon excited in a hollow cathode discharge. Ions formed by the focused laser beam in the mass spectrometer were subjected to two stages of acceleration prior to entering a field-free drift region and were detected by a channel electron multiplier (channeltron). The amplified output of the channeltron was monitored using a digital oscilloscope connected to a PC via an IEEE interface. To obtain mass selected REMPI spectra, the dye laser was scanned and only that part of the total ion signal that fell within a narrow time window centered on the TOF of the mass of interest was collected, averaged, and stored.

REMPI-PE spectra were obtained using an excimer pumped dye laser system with the laser output being frequency doubled when required and focused (f.l.=25 mm) into the ionization region of the magnetic bottle electron spectrometer. An effusive beam of pure CS_2 vapor was

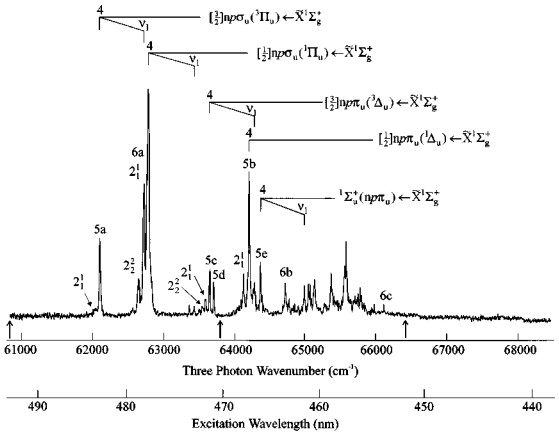

FIG. 1. 3+1 REMPI spectrum of a jet-cooled sample of CS_2 over the energy range 60 840–68 500 cm^{-1} recorded using linearly polarized light and monitoring only those ions with TOFs appropriate to m/z 76. This spectrum is a composite, obtained by splicing together spectra recorded using a number of different dyes. As discussed in the text, it was not possible to ensure correct normalization of the relative intensities of features appearing within the tuning range of any one dye, or between one dye tuning curve and the next. The vertical arrows arranged below the respective spectra indicate where the various scans have been joined. The $n=4$ members of the various $[^2\Pi_g]np\lambda_u \leftarrow \tilde{X}\ ^1\Sigma_g^+$ Rydberg series identified in Table I are indicated via the combs superimposed above the spectrum. The numbers above the various features (5a, 5b, etc.) refer to the photoelectron spectra recorded on these peaks and displayed in Figs. 5 and 6.

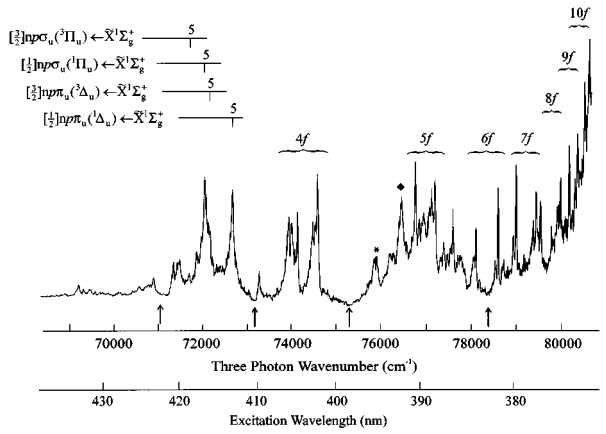

FIG. 2. 3+1 REMPI spectrum of a near room temperature sample of CS_2 over the energy range 68 400–81 000 cm^{-1} recorded using linearly polarized light and monitoring the total yield of photoelectrons. As with Fig. 1, this spectrum is a composite obtained by splicing together spectra recorded using a number of different dyes, and the same comments apply. Members of the various $[^2\Pi_g]np\lambda_u \leftarrow \tilde{X}\ ^1\Sigma_g^+$ Rydberg series and the $[^2\Pi_g]nf \leftarrow \tilde{X}\ ^1\Sigma_g^+$ complexes identified in Tables I and II are indicated via the combs and brackets festooned above the spectrum. The peaks identified by the symbols * and ♦ indicate atomic carbon and atomic sulphur resonances, respectively.

crossed by the focused laser beam and photoelectrons resulting from each laser pulse were extracted into the spectrometer. The measured times of arrival of the photoelectrons at a pair of microchannel plates situated at the end of the 500 mm flight tube were used to determine electron kinetic energies. A transient digitizer, interfaced to a PC, recorded preamplified output signals from the microchannel plates. Certain wavelength-resolved REMPI spectra were recorded in Amsterdam by measuring the total photoelectron yield as a function of excitation wavelength. Kinetic-energy-resolved photoelectron spectra were obtained by progressively stepping the retarding voltage on a grid in the flight tube and, at each voltage setting, performing a time-to-energy transformation on just the highest resolution (i.e., slowest) part of the TOF spectrum, with a resultant 15 meV (FWHM) resolution at all kinetic energies in the present experiments. Sulphur atoms were produced by CS_2 photolysis in the source region as a by-product of the REMPI process, and the measured electron kinetic energies from known S atom transitions[55,56] provided a convenient calibration that enabled the CS_2 photoelectron kinetic energies to be placed on an absolute scale. Alternatively, the CS_2 sample could be doped with xenon and well-documented REMPI transitions terminating on the two spin–orbit states of the Xe^+ ion were then used to calibrate the REMPI-PE spectra.

RESULTS AND DISCUSSION

REMPI Spectra

Figures 1 and 2 show the REMPI spectrum of CS_2, resonance enhanced at the three photon energy, recorded using linearly polarized laser radiation in the wavelength range 370–495 nm. The spectrum displayed in Fig. 1 was obtained using a jet-cooled sample and mass selective ion detection, monitoring just the parent ion peak (mass to charge ratio, m/z 76), while that shown in Fig. 2 (obtained using a thermal effusive source) involved measurement of the total photoelectron current as a function of excitation wavelength. Figures 3(a)–3(c) show the corresponding two photon resonance enhanced MPI spectrum of jet-cooled CS_2 molecules, again recorded using linearly polarized laser radiation and monitoring the wavelength dependence of the parent ion mass peak, this time in the range 355–247 nm. We comment that much of the structure evident in this spectrum at excitation wavelengths longer than 290 nm is actually due to 1+2 REMPI processes involving bent excited valence states of CS_2 whose spectroscopy has been investigated in earlier near uv absorption studies.[2,6,7,12] Inevitably, a number of dyes were required to achieve the wavelength coverage shown in each of these spectra: We have not taken any particular care about normalizing the laser power within the tuning range of any one dye, nor between successive dyes. Thus one should not give undue credence to the relative peak intensities, particularly those displayed in Figs. 1 and 3. Our focus here is primarily on the frequencies of the various resonances. Figure 4, which highlights the fact that ion fragmentation becomes far more prevalent at the shorter excitation wavelengths, illustrates a further reason for caution when interpreting the relative strengths of peaks appearing in mass selected excitation spectra such as those shown in Figs. 1 and 3. In fact, as Baker *et al.*[39] have demonstrated (and we confirm but do not show in Fig. 4), ion fragmentation can also give rise to local intensity variations in the mass selected REMPI spectrum of CS_2: The 3+1 REMPI spectrum shown in Fig. 1 provides an underestimate of the true strength of the

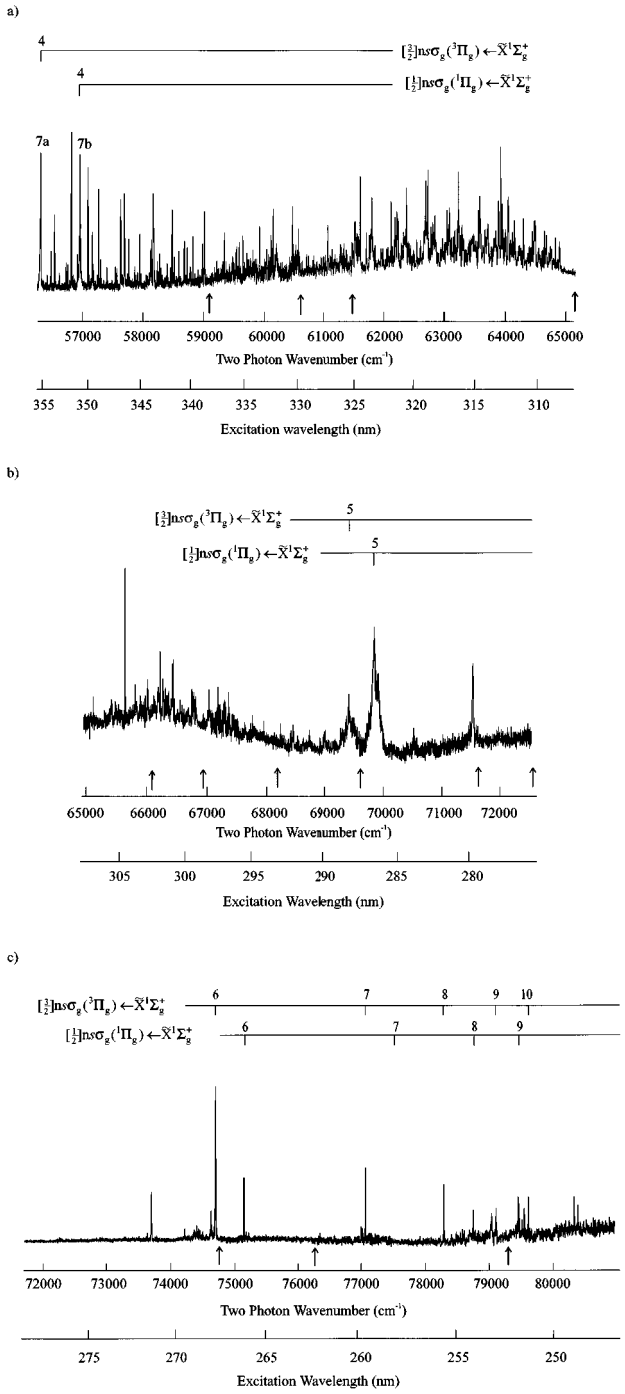

FIG. 3. 2+1 REMPI spectra of a jet-cooled sample of CS_2 over the energy range 56 500–81 000 cm^{-1} recorded using linearly polarized light and monitoring only those ions with times-of-flight appropriate to m/z 76. As in Fig. 1, the displayed spectra are composites, obtained by splicing together spectra recorded using a number of different dyes, and the same reservations about relative peak intensities apply. The vertical arrows arranged below the respective spectra indicate where the various scans have been joined. Members of the $[^2\Pi_g]ns\sigma_g \leftarrow \tilde{X}\ ^1\Sigma_g^+$ Rydberg series identified in Table III are indicated via the combs festooned above the spectrum. The two features which are the subject of the photoelectron spectra in Fig. 7 are indicated by the labels 7a and 7b.

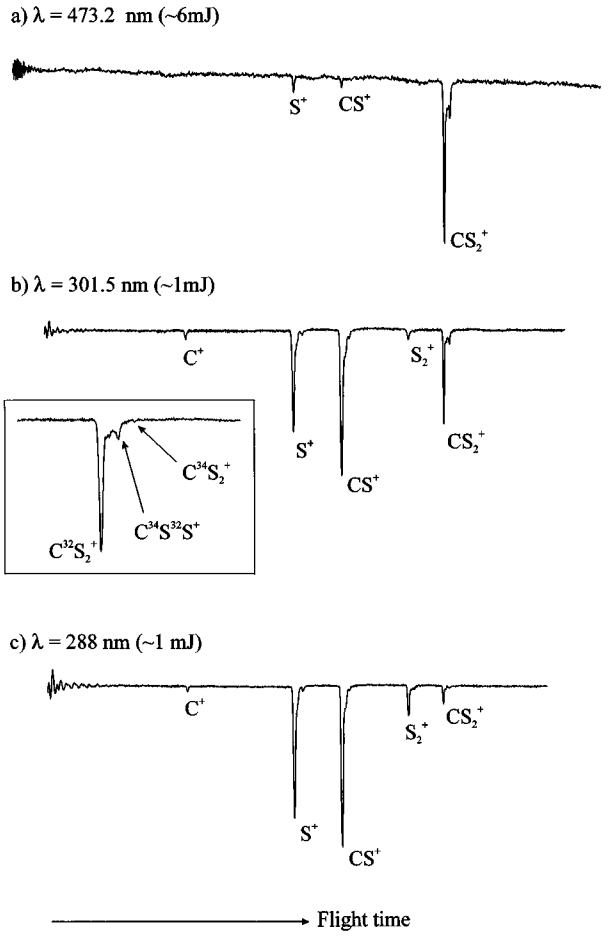

FIG. 4. Ion TOF spectra obtained following REMPI of CS_2 at (a) 473.2 nm, (b) 301.5 nm, and (c) 288 nm using laser pulse energies of 6, 1, and 1 mJ, respectively. These highlight the greatly increased propensity for ion fragmentation at the shorter excitation wavelengths. The inset to panel (b) illustrates TOF peaks associated with parent ions containing one and two ^{34}S nuclei.

64 209 cm^{-1} (64 214 cm^{-1} in Ref. 39) feature simply because, at the relevant excitation frequencies, an accidental one photon resonance in the CS_2^+ parent ion greatly enhances its probability of undergoing two photon dissociation (as evidenced by a dramatic increase in the S^+ and CS^+ fragment ion yields). The small shoulders evident on the high mass side of each of the major sulphur containing ions in Fig. 4 are due to the presence of the ^{34}S isotope (4.2% natural abundance); the finite TOF resolution at these higher ion masses, allied with the weakness of these features, prevented us from recording any worthwhile REMPI spectra associated with the heavier isotopomers. With the exception of the S_2 species, all of the other fragments were seen to exhibit some spectroscopy of their own: This we discuss later.

Photoelectron spectra

The kinetic energy resolution of the present REMPI-PES measurements (ca. 15 meV) is more than sufficient for us to be able to distinguish ionizations to the $^2\Pi_{g3/2}$ and $^2\Pi_{g1/2}$ spin–orbit components of the ground state ion (2 A$\sim$440 cm^{-1}, 54.6 meV).[34] For simplicity, these will henceforth be referred to simply as [3/2] and [1/2], respectively; when appropriate, these labels will also be used to indicate the ion

core involved in the various Rydberg states. Representative sets of REMPI-PE spectra are shown in Figs. 5–7 and will be considered in turn. The PE spectra shown in Fig. 5 all arise as a result of three photon resonant, four photon ionization processes. The first two both show one dominant peak, consistent with the final one photon ionization step from the resonance enhancing Rydberg state involving a $\Delta v=0$ transition (as expected on Franck–Condon grounds if the Rydberg state has a very similar geometry to that of the ion) to predominantly one of the two spin–orbit states of the ion. The first PE spectrum [Fig. 5(a)] was obtained following excitation at 483.1 nm ($3\tilde{\nu}=62\,100$ cm^{-1}); the kinetic energy of the major peak (0.188 eV) is consistent with ionization to the $v^+=0$ (shorthand notation for $v_1^+=v_2^+=v_3^+=0$) level of the lower, [3/2], spin–orbit component of the ion thus implying, by Franck–Condon arguments, that the resonance enhancement also involves an electronic origin, almost certainly that of a Rydberg state built on the [3/2] ion core. Such a conclusion is fully consistent with that reached in a number of previous analyses;[8,10,13,39] namely, that this feature should be assigned as the origin of the $[3/2]4p\sigma_u,(^3\Pi_u)\leftarrow\tilde{X}\ ^1\Sigma_g^+$ Rydberg transition. By way of contrast, Fig. 5(b) shows the complementary REMPI-PE spectrum that results when we excite at 467.2 nm ($3\tilde{\nu}=64\,209$ cm^{-1}), via the origin of a Rydberg state involving the [1/2] core. The measured photoelectron kinetic energies indicate that the resulting ions are formed in the $v^+=0$ level of the [1/2] spin–orbit state of the ion, thereby serving to confirm the recent assignment of this feature as the origin of the $[1/2]4p\pi_u,(^1\Delta_u)\leftarrow\tilde{X}\ ^1\Sigma_g^+$ Rydberg transition.[39,40]

Not all of the resonance enhancing levels ionize so ''cleanly'' as those shown in Figs. 5(a) and 5(b). Consider, for example, the features appearing at 471.4 and 471.0 nm ($3\tilde{\nu}=63\,644$ and $63\,700$ cm^{-1}, respectively), both of which have at various times[39,40] been assigned as the lower energy $[3/2]4p\pi_u,(^3\Delta_u)\leftarrow\tilde{X}\ ^1\Sigma_g^+$ counterpart of the $64\,209$ cm^{-1} resonance. The associated REMPI-PE spectra shown in Figs. 5(c) and 5(d) suggest a solution to the existing ambiguity. The former shows four peaks, the largest, fastest of which duly appears at a kinetic energy (0.443 eV) consistent with ionization to the [3/2], $v^+=0$ level of the ion. Ionization to the [1/2], $v^+=0$ level is seen to occur with only low probability, again consistent with the premise that the intermediate Rydberg state does indeed have a reasonably pure [3/2] ion core. What then should we make of the two additional peaks at 0.360 and 0.306 eV which, on energetic grounds, we associate with formation of ions with both [3/2] and [1/2] cores, each with ca. 650 cm^{-1} of internal energy? The photoelectron spectrum resulting from 3+1 REMPI via the neighboring $63\,700$ cm^{-1} feature [Fig. 5(d)] exhibits *the same peaks*, but the relative intensities of the ''fast'' and ''slow'' kinetic energy peaks are reversed. The obvious explanation, upon which we elaborate further in the later discussion, is that these two resonances are the result of vibronic mixing between two levels which, in zero order, should be viewed as (i) an electronic origin involving the [3/2] ion core and (ii) an excited level (carrying some 650 cm^{-1} of vibrational energy) built on a spin–orbit ''mixed'' core. Our final example in this panel [Fig. 5(e)] shows a further example of ionization from an intermediate state which appears to be built on a mixed ion core. This photoelectron spectrum was obtained following 3+1 REMPI at an excitation wavelength of 466.1 nm ($3\tilde{\nu}=64\,369$ cm^{-1}), a feature that has been tentatively assigned[39] as the origin of the $^1\Sigma_u^+\leftarrow\tilde{X}\ ^1\Sigma_g^+$ transition associated with the $4p\pi_u\leftarrow 2\pi_g$ Rydberg excitation. It is dominated by peaks indicative of ion formation in the $v^+=0$ levels of *both* spin–orbit states of the ion.

Figure 6 shows further examples of the way in which REMPI-PES can aid the assignment of individual vibronic features observed in the wavelength resolved REMPI spectra. Consider the three photon resonance evident in Fig. 1 at an excitation wavelength of 478.3 nm ($3\tilde{\nu}=62\,720$ cm^{-1}). Should we assign this as a transition involving a vibrationally excited level of the Rydberg state with origin at $62\,100$ cm^{-1}, carrying ca. 620 cm^{-1} of internal energy, or as a ''hot band'' associated with the Rydberg origin at $62\,780$ cm^{-1} (see Table II)? Analysis of the corresponding REMPI-PE spectrum [shown in Fig. 6(a)] helps to clarify the situation. The strongest peak in this photoelectron spectrum appears at a kinetic energy ca. 650 cm^{-1} lower than that associated with formation of the vibrationless [3/2] ground state ion, thus supporting the suggestion that the three photon resonance is indeed associated with a vibrationally excited level (1^1) of the Rydberg state whose origin occurs at $62\,100$ cm^{-1}. This explanation, however, does not account for the other significant peak appearing in Fig. 6(a), at a kinetic energy of 0.238 eV, just where we might expect to observe any $\Delta v=0$ ionizations to the [1/2] spin–orbit state of the ion. Thus we are able to confirm the recent suggestion[39] that the $62\,720$ cm^{-1} feature actually consists of two overlapping transitions (see Table II), one of which involves the $v_1=1$ level of the Rydberg state whose origin appears at $62\,100$ cm^{-1}, the other a hot band, most probably the 2_1^1 band (both on Boltzmann grounds and on the basis of the change in vibrational frequency upon exciting from the ground to the Rydberg state) of the Rydberg transition whose origin falls at $62\,780$ cm^{-1}.

Interpretation of the REMPI-PE spectra shown in Figs. 6(b) and 6(c), obtained following 3+1 REMPI at wavelengths of 463.5 and 453.7 nm ($3\tilde{\nu}=64\,724$ and $66\,119$ cm^{-1}, respectively), is less clear cut. In both cases the peaks corresponding to formation of $v^+=0$ ions are weak. The dominant feature in the former spectrum is a doublet, the kinetic energies of which (0.496 and 0.480 eV) are most readily interpretable in terms of formation of ions in their upper [1/2] spin–orbit state with ca. 590 and 710 cm^{-1} of internal energy. Additional, yet higher resolution REMPI-PES experiments will probably be needed in order to decide whether these internal energies should be associated with the formation of ions in one or more of the various Renner–Teller components associated with $v_2^+=2$ and/or with $v_1^+=1$. The dominant feature in Fig. 6(c) appears at a kinetic energy ca. 0.550 eV, some 243 meV (ca. 1960 cm^{-1}) below that of the peak associated with the formation of ions in their [1/2] spin–orbit state. The satellite feature at 0.608 eV shows

TABLE II. Wave numbers, effective quantum numbers (n^*) and proposed assignments for observed molecular CS_2 three-photon resonances to the $[^2\Pi_g]np$ Rydberg states. Values in parentheses correspond to the measurements of Baker *et al.* (Ref. 39).

$[\frac{3}{2}]np\sigma_u(^3\Pi_u)\leftarrow\tilde{X}\,^1\Sigma_g^+$				$[\frac{1}{2}]np\sigma_u(^1\Pi_u)\leftarrow\tilde{X}\,^1\Sigma_g^+$			
$\tilde{\nu}$ (cm^{-1})		Vibronic assignment	n^*	$\tilde{\nu}$ (cm^{-1})		Vibronic assignment	n^*
				62 563		2_3^3	
				62 647	(62 627)	2_2^2	
62 039	(62 013)	2_1^1		62 720	(62 704)	2_1^1	
62 100	(62 083)	Origin	2.39	62 780	(62 768)	Origin	2.40
				63 358	(63 352)	$2_1^1 1_0^1$	
62 720		1_0^1		63 424	(63 413)	1_0^1	
				63 495		2_0^2	
71 694		Origin	3.38	72 120		Origin	3.38
$[\frac{3}{2}]np\pi_u(^3\Delta_u)\leftarrow\tilde{X}\,^1\Sigma_g^+$				$[\frac{1}{2}]np\pi_u(^1\Delta_u)\leftarrow\tilde{X}\,^1\Sigma_g^+$			
$\tilde{\nu}$ (cm^{-1})		Vibronic assignment	n^*	$\tilde{\nu}$ (cm^{-1})		Vibronic assignment	n^*
63 544	(63 534)	2_2^2					
63 583	(63 578)	2_1^1		64 130		2_1^1	
63 644	(63 641)	Origin	2.49	64 209		Origin	2.50
64 280	(64 284)	1_0^1		64 724		+515 cm^{-1}	
				65 375		+1166 cm^{-1}	
				65 576		$2_0^2 1_0^1$	
				66 119		1_0^3	
72 168		Origin	3.47	72 666		Origin	3.48
				73 287		1_0^1	
$^3\Sigma_u^+(np\pi_u)\leftarrow\tilde{X}\,^1\Sigma_g^+$				$^1\Sigma_u^+(np\pi_u)\leftarrow\tilde{X}\,^1\Sigma_g^+$			
$\tilde{\nu}$ (cm^{-1})		Vibronic assignment		$\tilde{\nu}$ (cm^{-1})		Vibronic assignment	n^*
				64 369	(64 374)	Origin	2.55
				64 991		1_0^1	
63 700	(63 698)	2_0^2		65 050		2_0^2	
				65 763		$2_0^2 1_0^1$	

a similar energy shift from the peak we associate with ionization to the origin level of the [3/2] spin–orbit state of the ion. Such observations would be explicable if we assign the 66 119 cm^{-1} resonance in terms of excitation to a vibrationally excited level of a Rydberg state built (predominantly) on the [1/2] ion core. The vibrational energy in the ion (1960 cm^{-1}) is most readily interpretable as three quanta of the symmetric stretching mode ν_1. We note that the 66 119 cm^{-1} feature in Fig. 1 exhibits a similar shift from the intense band at 64 209 cm^{-1} [the associated REMPI-PE spectrum for which was featured in Fig. 5(b)]. It is thus tempting to assign the former resonance as the 1_0^3 vibronic band associated with the Rydberg transition whose origin appears at 64 209 cm^{-1} (see Table II), but inspection of either Fig. 1 or the entries included in Table II leaves some concerns as to the location of the corresponding 1_0^1 and 1_0^2 bands.

Our final two examples of REMPI-PE spectra are displayed in Fig. 7. These two spectra were obtained following excitation at 355.2 nm ($2\,\tilde{\nu}$=56 312 cm^{-1}) and 351.1 nm ($2\,\tilde{\nu}$=56 965 cm^{-1}), respectively. Both excitations are consistent with two photon resonant, three photon ionization processes and were assigned as, respectively, the $[3/2]4s\sigma_g,(^3\Pi_g)$ and $[1/2]4s\sigma_g,(^1\Pi_g)$ Rydberg origins in the earlier 2+1 REMPI study of Couris *et al.*[36] At first sight, the complexity of their associated REMPI-PE spectra might cause one to doubt such assignments but, in fact, the present work confirms that these resonances are, indeed, Rydberg origin bands. The explanation for the apparent complexity of the REMPI-PE spectra rests on a chance coincidence between the energy separation of these two resonances (653 cm^{-1}) and the wave number of the symmetric stretching vibration, ν_1 (~640 cm^{-1} in the ground and Rydberg states of the neutral, and in the ground state of the ion). Consider first the photoelectron spectrum accompanying 2+1 REMPI of CS_2 at 355.2 nm [Fig. 7(a)]. As the supporting energy level diagram illustrates, peaks *b* and *a* are consistent with two photon excitation from the ground state to the $[3/2]4s\sigma_g$ Rydberg origin, followed by a further one photon ionization to the zero-point vibrational levels of both the [3/2] and [1/2]

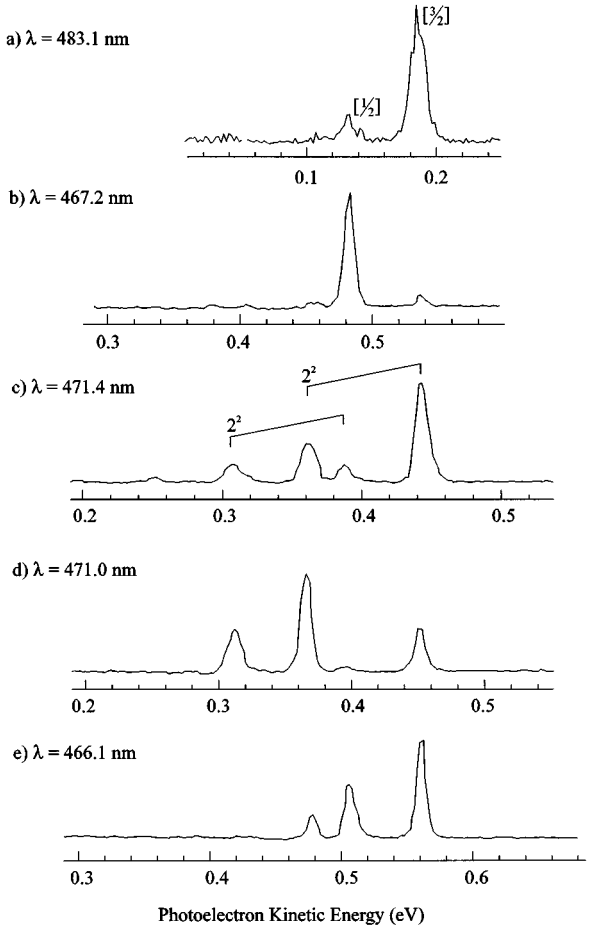

FIG. 5. Illustrative REMPI-PE spectra of CS_2 obtained following excitation at (a) 483.1 nm, where we excite a three photon resonance ($3\tilde{\nu}$=62 100 cm^{-1}) involving the zero-point level of the $[3/2]4p\pi_u,(^3\Pi_u)$ Rydberg state, (b) 467.2 nm ($3\tilde{\nu}$=64 209 cm^{-1}), where the resonance enhancement is provided by the $[1/2]4p\pi_u,(^1\Delta_u)$ Rydberg origin and the kinetic energy of the dominant photoelectron peak indicates that the partner ion is formed in the ground ($v^+=0$) level of the upper [1/2] spin–orbit state; (c) 471.4 nm ($3\tilde{\nu}$ =63 644 cm^{-1}) and (d) 471.0 nm ($3\tilde{\nu}$=63 700 cm^{-1})— resonances which we attribute to the result of vibronic mixing between two states which, in zero-order, would be described as the $[3/2]4p\pi_u,(^3\Delta_u)$ Rydberg origin and the Δ component of the 2^2 vibrational level associated with the $[3/2]4p\pi_u,(^3\Sigma_u^+)$ state—see the text for further details; (e) 466.1 nm ($3\tilde{\nu}$=64 369 cm^{-1}) involving the $[1/2]4p\pi_u,(^1\Sigma_u^+)$ origin level which shows ionization to both spin–orbit components of the ion. The kinetic energy scales have been offset so that the various vibronic states of the ion align vertically.

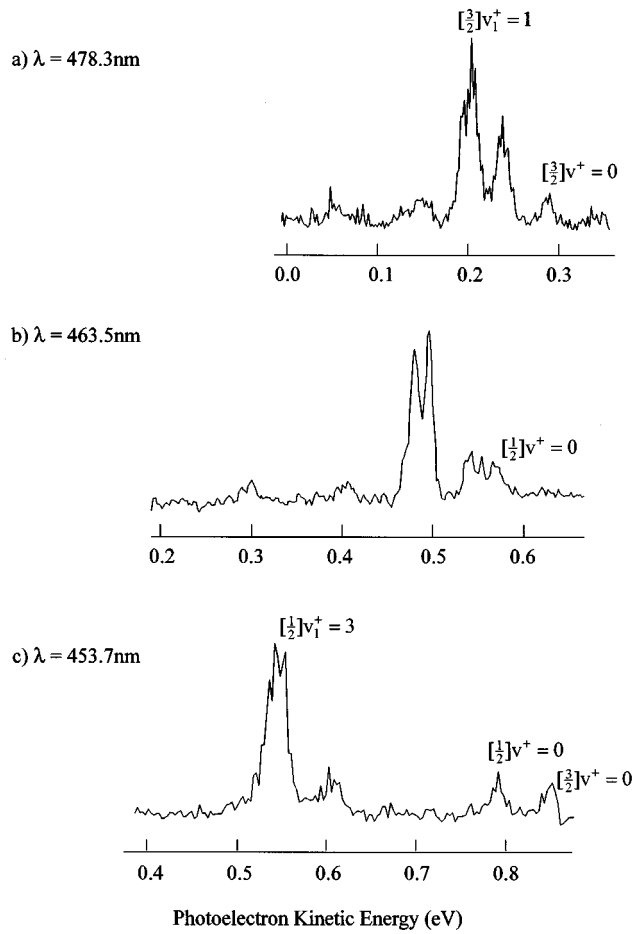

FIG. 6. MPI-PE spectra of CS_2 obtained following excitation at (a) 478.3 nm ($3\tilde{\nu}$=62 720 cm^{-1}). On the basis of the measured photoelectron kinetic energies we deduce this three photon resonance to be a blend of two transitions; the 1_0^1 band of the $[3/2]4p\sigma_u,(^3\Pi_u)\leftarrow\tilde{X}\ ^1\Sigma_g^+$ Rydberg transition, and the 2_1^1 hot band of the corresponding $[1/2]4p\sigma_u,(^1\Pi_u)\leftarrow\tilde{X}\ ^1\Sigma_g^+$ excitation; (b) 463.5 nm ($3\tilde{\nu}$=64 724 cm^{-1}), where the kinetic energies of the dominant photoelectron peaks are consistent with the partner ion being formed in its [1/2] spin–orbit state with ca. 590 and 710 cm^{-1} of vibrational energy; and (c) 453.7 nm ($3\tilde{\nu}$=66 119 cm^{-1}), where the kinetic energy of the dominant photoelectron peak is consistent with the partner ion being formed in its [1/2] spin–orbit state with ca. 1960 cm^{-1} of vibrational energy. As in Fig. 5, the kinetic energy scales have been offset so that the various vibronic states of the ion align vertically.

spin–orbit states of the ion, thus implying that the ion core involved in this particular Rydberg state may be less ''pure'' than indicated by the state label used here. To account for the faster peaks [*d* and *c* in Fig. 7(a), with kinetic energies of 0.475 and 0.419 eV, respectively] it is necessary to invoke a hot band transition, namely, two photon excitation from the $v_1=1$ level of the ground state to the $[1/2]4s\sigma_g$ Rydberg origin (which because of the accidental near degeneracy is likely to be overlapped by, and quite possible mixed with, the $[3/2]4s\sigma_g$, $v_1=1$ level), followed by ionization terminating on the same zero-point levels of the ion. Note that, because of this accidental degeneracy and given the resolution of the present REMPI-PES experiments, any one photon ionization from the $[3/2]4s\sigma_g,v_1=1$ level terminating on the $v_1^+=1$ levels of the ion (which, on Franck–Condon grounds, would be expected to be quite significant) will simply reinforce peaks *a* and *b*. The 2+1 REMPI-PE spectrum taken at 351.1 nm [Fig. 7(b)] provides further evidence of the accidental degeneracy between the $[3/2]4s\sigma_g,v_1=1$ and $[1/2]4s\sigma_g,v=0$ levels of CS_2. In this case, the initial two photon excitation is from the ground vibrational level to the overlapping and/or mixed $[1/2]4s\sigma_g$, $v=0$ and $[3/2]4s\sigma_g,v_1=1$ Rydberg levels; the energies of the main peaks evident in the REMPI-PE spectrum are consistent with ion formation in the $v^+=0$ (peaks *h* and *e*) and $v_1^+=1$ levels (peaks *f* and *g*) of both spin–orbit states of the ground state ion.

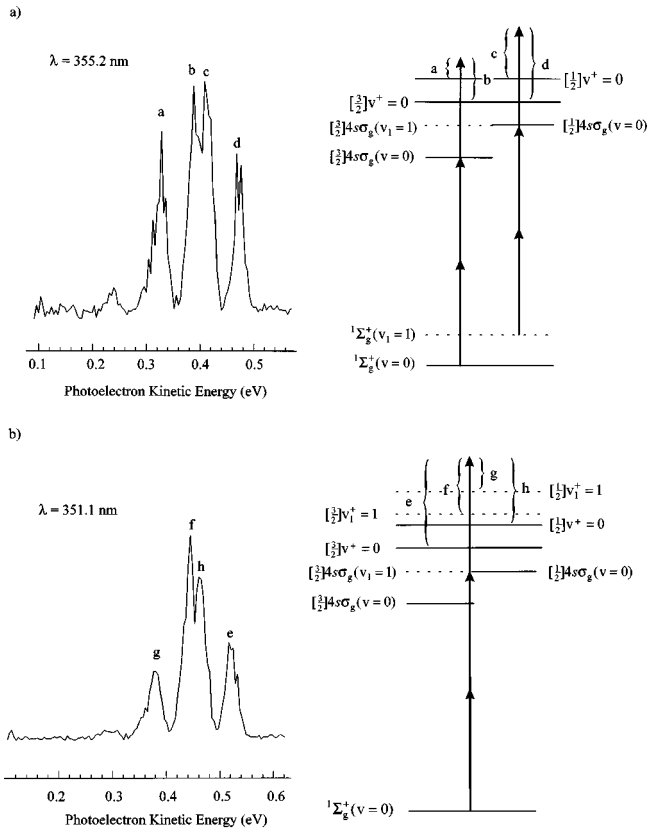

FIG. 7. 2+1 REMPI-PE spectra of CS_2 obtained following excitation of what, at first glance, might appear to be just the two spin–orbit components of the $[^2\Pi_g]4s\sigma_g \leftarrow \tilde{X}\ ^1\Sigma_g^+$ Rydberg origin at (a) 355.2 nm ($2\tilde{\nu}$=56 312 cm^{-1}) and (b) 351.1 nm ($2\ \tilde{\nu}$=56 965 cm^{-1}). The accompanying schematic energy level diagrams provide an explanation for the unexpectedly complex appearance of these two REMPI-PE spectra. (See the text for further details.)

Assigning the multiphoton resonances

Band maxima ($\tilde{\nu}$) for the features identified in this work are listed in Tables II–IV together with, when appropriate, their quantum defect (δ) and/or the effective quantum number [$(n^*=n-\delta)$, where n is the principal quantum number] calculated using the relationship

$$\tilde{\nu} = E_i - R/(n^*)^2, \tag{2}$$

where E_1=81 286 or 81 726 cm^{-1} according to whether the Rydberg state belongs to a series converging to the [3/2] or [1/2] spin–orbit component of the ion, and R is the Rydberg constant (109 737 cm^{-1}). For completeness, we also list the major peaks identified in the recent multiphoton studies.[36–40]

Before discussing and assigning the resonances observed in Figs. 1–3 we should consider one aspect of nomenclature, namely, the most appropriate labeling scheme for the various Rydberg states. Consider, for example, the Rydberg states derived from the configuration $\cdots(2\pi_g)^3(4s\sigma_g)$.[1] In what follows we generally choose to adopt a Hund's case (c) coupling scheme in which we explicitly separate the angular momentum of the ion core, $\Omega_c=\frac{3}{2}$ or $\frac{1}{2}$, from that of the Rydberg electron, whereas most previous workers have chosen to label these same excited states using the labels appropriate to a Russell–Saunders, or Λ, S, coupling scheme, viz., $^3\Pi_g$ and $^1\Pi_g$. Figure 8 shows the correlation between these two limits, and highlights the fact that it is the relative magnitudes of the exchange energy, K, and the spin–orbit coupling constant, A, that determine which is the more appropriate.[57] Clearly, in the limit of high n, as K tends to zero and in the absence of any clearly resolved rotational fine structure, it must be most appropriate to use the Hund's case (c) scheme adopted in this work.

We now turn to discuss the various spectral features observed in the present REMPI work. Recalling Table I we recognize that, by virtue of the fact that CS_2 is centrosymmetric, the present 3+1 and 2+1 REMPI spectra originating from the $\tilde{X}\ ^1\Sigma_g^+$ ground state should provide complementary information (relating to, respectively, the ungerade and gerade excited states). For organizational simplicity we therefore choose to consider these two sets of transitions in turn.

TABLE III. Observed molecular CS_2 three-photon resonances to the $[^2\Pi_g]nf$ Rydberg states. The wave numbers given are for the center of each particular band. Ω^+ represents the dominant ion core configuration as revealed by the REMPI-PE spectra.

$\tilde{\nu}$ (cm^{-1})	n	Ω^+
74 016	4	3/2
74 532		1/2
76 730	5	3/2
77 160		1/2
78 144	6	3/2
78 570		1/2
78 969	7	3/2
79 440		1/2
79 536	8	3/2
79 980		1/2
79 902	9	3/2
80 352		1/2
80 172	10	3/2
80 610		1/2

TABLE IV. Wave numbers, principal quantum number (n), and vibronic assignments when not an electronic origin, and quantum defects (δ) for the presumed $[^2\Pi_g]ns\sigma_g$ Rydberg states. The values in parentheses correspond to the measurements of Couris *et al.* (Ref. 36). Those positions indicated with an asterisk are very weak and only observable via electron detection (see Fig. 10).

$[3/2]ns\sigma_g(^3\Pi_g) \leftarrow \tilde{X}\ ^1\Sigma_g^+$			$[1/2]ns\sigma_g(^1\Pi_g) \leftarrow \tilde{X}\ ^1\Sigma_g^+$		
$\tilde{\nu}$ (cm^{-1})	n	δ	$\tilde{\nu}$ (cm^{-1})	n	δ
56 312	4	1.91	56 965	4	1.90
(56 315)			(56 974)		
69 414	5	1.96	69 847	5	1.96
74 628	6 (2_1^1)		75 080*	6 (2_1^1)	
74 701	6	1.92	75 151	6	1.91
75 378*	6 (1_0^1)		75 810*	6 (1_0^1)	
76 998	7 (2_1^1)		77 436*	7 (2_1^1)	
77 061	7	1.90	77 496*	7	1.91
78 293	8	1.95	78 756	8	1.92
79 112	9	1.89	79 550	9	1.90
79 624	10	1.88			

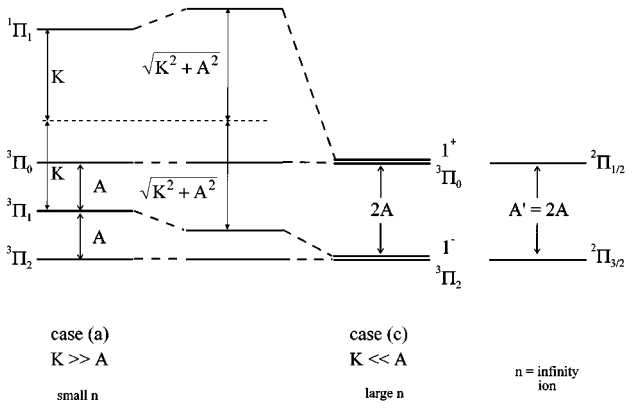

FIG. 8. Diagram showing the correlations between states arising from a $\pi^3\sigma^1$ configuration when using the alternative Λ, S [Russell–Saunders, or case (a)] and Ω_c, ω [case (c)] coupling schemes. The level labels 1^+ and 1^- denote $|1^{\pm}\rangle = (1/\sqrt{2})[|^3\Pi_1\rangle \pm |^1\Pi_1\rangle]$ as discussed in Ref. 57.

Three photon resonances

The 61 000–67 000 cm^{-1} region shown in Fig. 1 has been the subject of many previous experimental investigations, involving both one photon absorption spectroscopy[1,5,8,13,14] and multiphoton excitation methods,[37–40] but the assignment of the observed resonances has remained a matter of some controversy. Guided by symmetry and quantum defect considerations, by our analyses of the accompanying REMPI-PE spectra, and in accord with the conclusions of several of the earlier one photon absorption[5,8,13] and the more recent REMPI studies,[39,40] we assign the three photon resonances centered at 62 100 and 62 780 cm^{-1} as the electronic origins of the first ($n=4$) members of the $[3/2]np\sigma_u,(^3\Pi_u)\leftarrow\widetilde{X}\ ^1\Sigma_g^+$ and $[1/2]np\sigma_u,(^1\Pi_u)\leftarrow\widetilde{X}\ ^1\Sigma_g^+$ series. Both of these features were also evident in the earlier 3+1 REMPI spectrum reported by Li *et al.*;[37] these workers adopted the same interpretation for the higher energy feature, but offered no assignment for the 62 100 cm^{-1} resonance. Magnetic circular dichroism measurements[58] also support the assignment of the 62 780 cm^{-1} feature in terms of a perpendicular transition, but this same group chose to assign the 62 100 cm^{-1} transition as a hot band—a suggestion which the present REMPI-PE spectra unambiguously refute. The quantum defects for these two states (δ=1.61 and 1.60, respectively, assuming that $n=4$) are entirely consistent with their assignment in terms of excitation to a p Rydberg orbital.

A more serious point of contention in this region of the 3+1 REMPI spectrum concerns the assignment of the two strong resonances centered at 63 644 and 64 209 cm^{-1}. Having previously identified *two* photon resonances [by two color $(1+1')+1$ REMPI spectroscopy[38]] which they assigned in terms of the $[3/2]3d\delta_g,(^3\Delta_g)\leftarrow\widetilde{X}\ ^1\Sigma_g^+$ and $[1/2]3d\delta_g,(^1\Delta_g)\leftarrow\widetilde{X}\ ^1\Sigma_g^+$ Rydberg excitations in this energy region, Li *et al.*[37,38] chose to assign these features in terms of transitions to excited levels of these gerade electronic states carrying one quantum of the π_u bending vibration, ν_2. REMPI-PES offers a means of testing these assignments and, in this particular case, as Figs. 5(b) and 5(c) showed, of disproving them. Both features correspond to electronic origin transitions, ionizing (predominantly) to the [3/2] and (cleanly) to the [1/2] states of the ion, respectively. The quantum defects of the two features ($\delta\sim$1.5, assuming $n=4$) suggest that these are the first members of another p Rydberg series, presumably ones based on the configuration $[^2\Pi_g]4p\pi_u$. Since these features have no obvious counterparts in the one photon absorption spectrum[1,5,8] it is tempting to suggest that they arise as a result of excitations to states with $\Omega_{\text{total}}>1$, most probably states which, in the language of (Λ, S) coupling, would be described using the term symbols $^3\Delta_u$ and $^1\Delta_u$. Baker and co-workers[39,40] have reached broadly similar conclusions, though the apparent splitting of the origin at lower energy remained something of a puzzle. These workers initially assigned the feature at 63 644 cm^{-1} as the 2_1^1 hot band of an electronic origin at 63 700 cm^{-1} [39] but this assignment was revised in their subsequent two-color[40] study in favor of an interpretation in which both of these features were due to origin bands. As we have seen, the present photoelectron spectra [Figs. 5(c) and 5(d)] suggest that these two closely spaced features are best pictured as arising from vibronic mixing between two zero-order states, one of which is the $[3/2]4p\pi_u,(^3\Delta_u)$ origin level, while the other is built on a spin–orbit mixed core and involves some 650 cm^{-1} of internal energy. Given the expected energetic ordering of the various (Λ,S) states derived from the configuration $(2\pi_g)^3(4p\pi_u)^1$—viz., $^1\Sigma_u^+$, $^1\Delta_u$, $^1\Sigma_u^-$, $^3\Sigma_u^-$, $^3\Delta_u$, and $^3\Sigma_u^+$, in order of decreasing energy[57]—and the fact that the two zero-order states must have the same *vibronic* symmetry, we suggest the 2^2 level of the hitherto unobserved $[3/2]4p\pi_u,(^3\Sigma_u^+)$ state as the most plausible assignment for the other zero-order state, and that this borrows intensity from mixing with the $[3/2]4p\pi_u,(^3\Delta_u)$ origin level. Such an assignment implies a term value ca. 63 050 cm^{-1} for the $[3/2]4p\pi_u,(^3\Sigma_u^+)$ origin. Core mixing appears to be a characteristic of the Σ_u members of the $[^2\Pi_g]4p\pi_u$ Rydberg complex: Recall that the photoelectron spectrum [Fig. 5(e)] obtained following 3+1 REMPI via the 64 369 cm^{-1} resonance which, in accord with Baker *et al.*[39,40] we assign as the origin of the $[^2\Pi_g]4p\pi_u(^1\Sigma_u^+)\leftarrow\widetilde{X}\ ^1\Sigma_g^+$ transition, also showed clear evidence for formation of $v^+=0$ ions in both spin–orbit states.

Of all the Rydberg states identified in this study, it is the pair of features at 56 312 and 56 965 cm^{-1} attributable to the excited configuration $[^2\Pi_g]4s\sigma_g$, and the pairs of states derived from the respective configurations $[^2\Pi_g]4p\sigma_u$ and $[^2\Pi_g]4p\pi_u$ that least conform to the Hund's case (c) labeling scheme. In each case the measured energy separation is substantially greater than the 440 cm^{-1} spin–orbit splitting in the ground state ion, implying a significant contribution from the exchange energy. This is as is to be expected, since it is in these lowest energy Rydberg states that the Rydberg electron will show the greatest core penetration and thus that the exchange interaction with the core should be greatest. We can gain some estimate for the magnitude of K in each of these cases if we assume the simple two state interaction model implied by Fig. 8, i.e., if we assume that the only interaction is between states belonging to the same $[^2\Pi_g]nl\lambda$

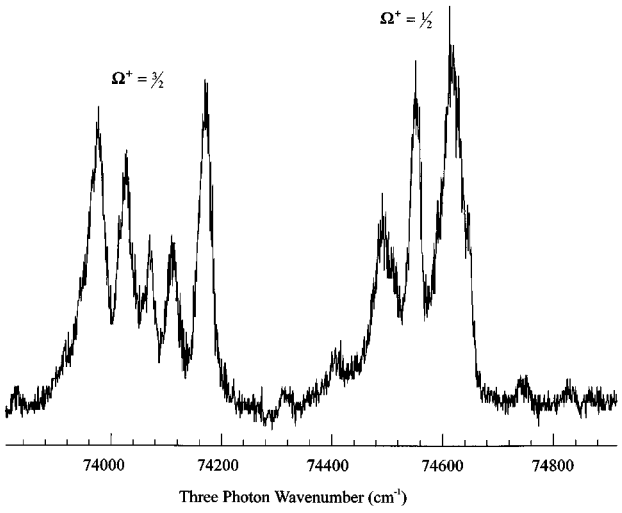

FIG. 9. Detail of the 73 800–74 900 cm^{-1} region of the 3+1 REMPI spectrum of CS_2, obtained by monitoring the yield of parent ions, showing the $[^2\Pi_g]4f \leftarrow \tilde{X}\ ^1\Sigma_g^+$ Rydberg complex. Ω^+ represents the dominant ion core configuration.

Rydberg complex and with a common Ω. Such a model implies values of K in the range 240–260 cm^{-1}.

As Table II shows, most of the other significant features we identify in the 61 000–67 000 cm^{-1} region of the 3+1 REMPI spectrum of CS_2 with the aid of REMPI-PES can be plausibly assigned in terms of transitions involving vibrationally excited states built upon the various recognized $[^2\Pi_g]4p\lambda_u \leftarrow \tilde{X}\ ^1\Sigma_g^+$ origins. Moving to higher energies (Fig. 2), we identify strong 3+1 MPI resonances attributable to most of the corresponding spin–orbit split $[^2\Pi_g]5p\lambda_u \leftarrow \tilde{X}\ ^1\Sigma_g^+$ origins (see Table II). We note that these assignments represent a substantial refinement over those derived from previous analysis of the room temperature one photon vuv absorption spectrum.[8] Our inability to observe any higher ($n>5$) members of these Rydberg series in the 3+1 REMPI spectrum suggests that, as in CO_2,[46] predissociation becomes increasingly efficient as we ascend in n (and in energy).

Above 74 000 cm^{-1} the 3+1 REMPI spectrum of CS_2 shows a dense progression of sharp bands which can be arranged into clumps which fit into two well defined series, split by ca. 440 cm^{-1}, converging to the two spin–orbit components of the ground state ion (see Table III). The accompanying REMPI-PE spectra show these to be origin transitions, while the fact that these series members are not apparent in the one photon absorption spectrum[1,5,8] and comparison with the findings of recent REMPI studies of CO_2,[46] both point to their assignment in terms of $[^2\Pi_g]nf \leftarrow \tilde{X}\ ^1\Sigma_g^+$ Rydberg members as indicated in Fig. 2 and in Table III. Such a view is reinforced by the clear similarities between the structure of the $[^2\Pi_g]4f \leftarrow \tilde{X}\ ^1\Sigma_g^+$ Rydberg complex shown in Fig. 9 and the band contours of the corresponding $[^2\Pi_g]nf \leftarrow \tilde{X}\ ^1\Sigma_g^+$ Rydberg complexes in CO_2 calculated using a Hund's case (e) representation.[47]

Two photon resonances

Figure 3 illustrated the fact that the lower energy part (wavelengths larger than 290 nm) of the mass resolved 2+1 REMPI spectrum of CS_2 is greatly complicated by the presence of overlapping features due to valence excitations resonant at the one photon energy (i.e., 1+2 REMPI transitions). This near uv region of the one photon absorption spectrum of CS_2 has been the subject of fairly detailed investigations in the past[2,6,7,12] and the positions of many of the more prominent band heads are well documented.[2,7] REMPI spectroscopy, when allied with the facility to measure photoelectron kinetic energies, provides a particularly straightforward and convenient means of distinguishing the 1+2 and 2+1 resonances in this spectral region. This selectivity arises as a result of the differing equilibrium geometries of the states resonant at the one and two photon energies. The two photon resonances involve linear Rydberg states with little vibrational excitation; their subsequent one photon ionization tends to be vibrationally adiabatic (recall Figs. 5–7) and the kinetic energies of the resulting photoelectrons generally approach the limiting values allowed by energy conservation. In contrast, the one photon resonances involve bent valence states with equilibrium geometries very different from that of the (linear) ground state ion. Thus the Franck–Condon factors associated with the subsequent two photon ionization step will favor population of a wide spread of (excited) vibrational levels of the ion, and the accompany photoelectrons will have correspondingly less kinetic energy.

This selectivity is illustrated in Fig. 10: The upper spectrum, an expanded portion of the spectrum shown in Fig. 3 taken using mass selective detection of the parent ions (m/z 76), contains both one and two photon resonances while the lower spectrum, obtained by monitoring just those photoelectrons with kinetic energies greater than ca. 0.35 eV, shows only the two photon resonances reported previously by Couris *et al.*[36] The different spectral widths of these features in the two spectra are largely attributable to the broader rotational envelope associated with the near room temperature sample used in the REMPI-PES study. Analyses of the photoelectron spectra accompanying these two resonances (Fig. 7), and the deduced quantum defects of these two bands ($\delta \sim 1.9$, assuming $n=4$), are both consistent with previous assignments that these two features correspond to the $[3/2]4s\sigma_g, (^3\Pi_g) \leftarrow \tilde{X}\ ^1\Sigma_g^+$ and $[1/2]4s\sigma_g, (^1\Pi_g) \leftarrow \tilde{X}\ ^1\Sigma_g^+$ Rydberg origins, respectively. Several features which can be plausibly assigned as higher members of these two series are clearly identifiable in Fig. 3, though the $n=5$ members (centered at ca. 69 414 and 69 847 cm^{-1}) appear surprisingly broad (perhaps on account of a reduced lifetime as a consequence of predissociation). Additionally, the $n=7$ member of the latter series appears anomalously weak and, as Fig. 11 shows, was in fact only identified in the spectrum recorded using photoelectron (rather than ion) detection; these various origins are listed in Table IV.

Finally we comment on the d Rydberg origin identified at 63 323 cm^{-1} in the previous two color $(1+1')+1$ REMPI study.[38] This region of the 2+1 REMPI spectrum of CS_2 is

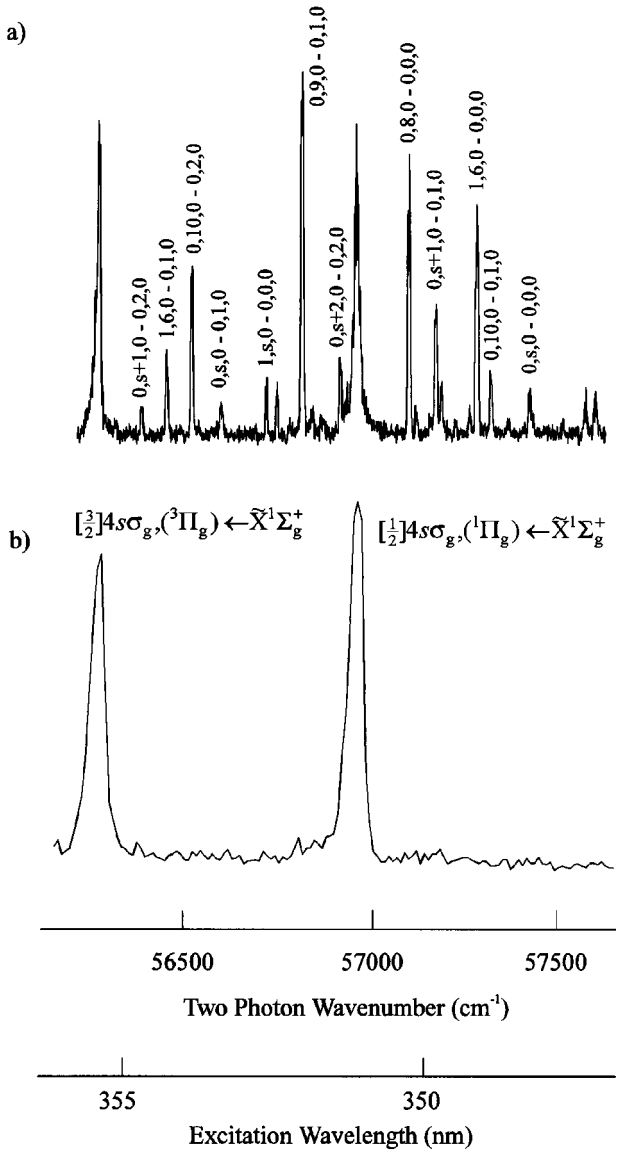

FIG. 10. Detail of part of the overall three photon ionization spectrum of CS_2 obtained by monitoring (a) the yield of parent ions, and (b) the yield of photoelectrons with kinetic energies greater than ca. 0.35 eV, as a function of excitation wavelength. As discussed in the text, the former spectrum (a) contains a superposition of one and two photon resonances associated with excitations to bent valence states and linear Rydberg states, respectively, while, because of the photoelectron kinetic energy chosen, only the latter contribute in spectrum (b). The vibronic assignments indicated in (a) are taken from Ref. 2.

heavily congested by the overlapping one photon resonances associated with vibronic levels of the bent valence states, to the extent that we were unable to identify this feature in the present work, even with the potential discrimination afforded by monitoring just a kinetic energy selected portion of the total photoelectron yield. This we attribute to a combination of spectral congestion and the weakness of the two photon REMPI transition via this $[^2\Pi_g]3d\leftarrow\tilde{X}\ ^1\Sigma_g^+$ Rydberg origin—presumably, as with the $[^2\Pi_g]np$ Rydberg states, because the resonance enhancing excited state is predissociated. Note that, in contrast to the work of Li *et al.*,[38] we see no unequivocal evidence for any vibronically induced (electronically forbidden) multiphoton excitations in the present spectra though a few significant features, listed in Table V, remain unassigned, most notably the prominent resonance observed following excitation at 279.6 nm ($2\tilde{\nu}$=71 533 cm^{-1}) which the accompanying REMPI-PE spectrum suggests is an electronic origin.

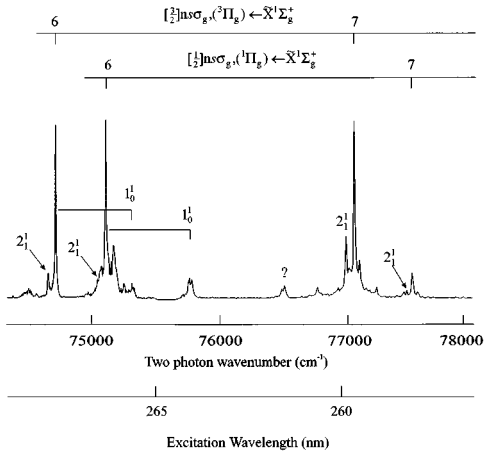

FIG. 11. Detail of the 74 500–78 000 cm^{-1} region of the 2+1 REMPI spectrum of a room temperature sample of CS_2 obtained by monitoring the total photoelectron current as a function of excitation wavelength which serves to highlight the anomalous weakness of the $[1/2]7s\sigma_g$, $(^1\Pi_g)\leftarrow\tilde{X}\ ^1\Sigma_g^+$ resonance.

Fragmentation of CS_2

As commented earlier, REMPI spectra obtained by monitoring the m/z 12, 32, and 44 mass channels each show structure that is clearly different from that associated with formation of the parent ion, thus indicating the formation of (and subsequent REMPI of) neutral C, S, and CS fragments in the present experiments. Figure 12 shows one of the more prominent features appearing in the m/z 44 mass channel—a blue degraded band which, by comparison with the earlier work of Ono and Hardwick,[59] we attribute to a 1+1 REMPI process in which the first step corresponds to the (0–1) and, at the shorter wavelength end, the overlapping (1–2) band of the $CS(^3\Sigma^+\leftarrow a\ ^3\Pi)$ transition. Energetic considerations sug-

TABLE V. Wave numbers, ion core symmetry, and effective quantum numbers (n^*) for unassigned two and three photon resonances. REMPI-PE spectroscopy indicates that all these resonance enhancements involve electronic origins save for the 74 128 cm^{-1} feature which was too weak to record a meaningful photoelectron spectrum.

$\tilde{\nu}$ (cm^{-1})	Ion core	n^*	3+1/2+1
68 946	[3/2]	2.98	3
69 246	[1/2]	2.97	3
70 911	[1/2]	3.18	3
71 533	[1/2]	3.28	2
73 696	[3/2]	3.80	2
74 010	[1/2]	3.77	3
74 128			2
75 780	[1/2]	4.29	2 (v.weak)
76 520	[3/2]	4.80	2 (v.weak)

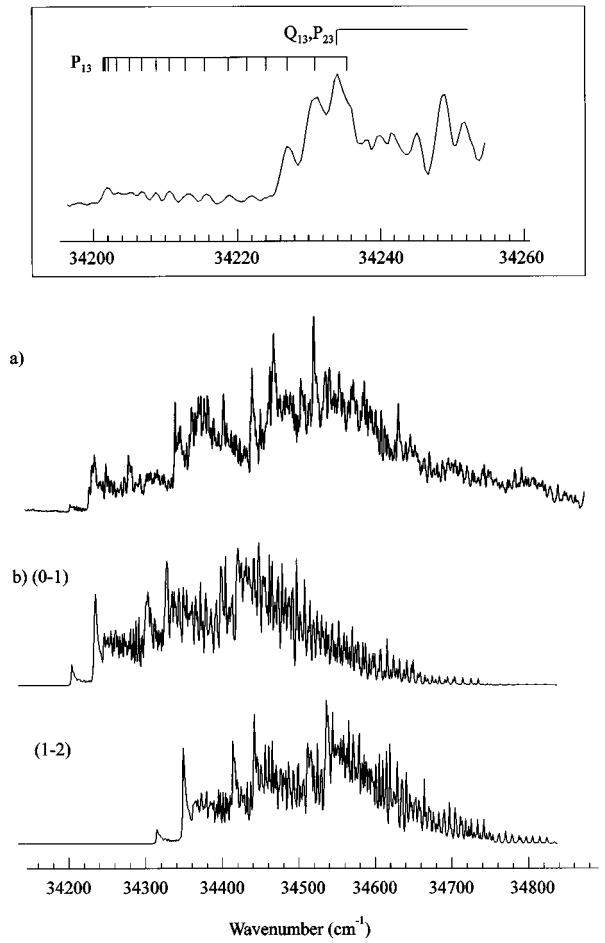

FIG. 12. (a) 1+1 REMPI spectrum showing the region of the $\Delta v=-1$ bands associated with the $^3\Sigma^+\leftarrow a\ ^3\Pi$ transition of the CS($a\ ^3\Pi$) fragments formed by two photon dissociation of a jet-cooled sample of CS_2 at the same excitation wavelengths. (b) Crude simulations of the (0–1) and (1–2) bands which assume spectroscopic parameters as given in Refs. 59 and 60, a laser linewidth of 0.4 cm^{-1} and a rotational temperature of 2000 K. These simulations are merely intended to demonstrate that the breadth of the observed spectrum can only be accommodated by assuming the CS($a\ ^3\Pi$) fragments to be formed with substantial rotational (and vibrational) excitation. The inset to panel (a) shows the low energy region of this band, with the combs indicating the assignments of Ono and Hardwick (Ref. 59).

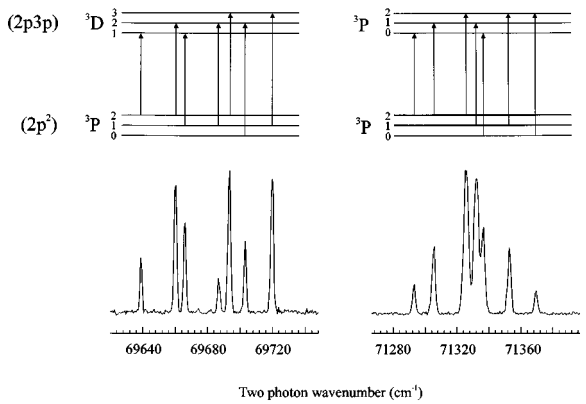

FIG. 13. 2+1 REMPI spectra of ground state C(^3P_J) atoms arising in the multiphoton excitation/ionization of CS_2, together with schematic energy level diagrams illustrating the source of the various multiplet splittings.

gest that these CS($a\ ^3\Pi$) fragments arise as a result of the following spin-allowed two photon dissociation:

$$CS_2 \rightarrow CS(a\ ^3\Pi) + S(^3P_J) \tag{3}$$

the thermochemical threshold for which is ca. 63 500 cm^{-1}.[9] Black *et al.*[18] have reported the excitation spectrum for forming electronically excited CS($a\ ^3\Pi$) fragments in the one photon dissociation of CS_2 and shown that the quantum yield for process (3) rises sharply as soon as the energetic threshold ($\lambda\sim158$ nm) is exceeded. The present observations of structured resonances in the region expected for the $\Delta v=-2$, -1, and 0 transitions of the CS($^3\Sigma^+\leftarrow a\ ^3\Pi$) transition (centered around excitation wavelengths of 300, and 291, and 282 nm, respectively) indicates the following: First, it suggests that the same dissociation channel can be reached via both one and two photon absorptions. Second, it provides some clues about the energy disposal in the fragments and thence about the photodissociation dynamics. As Fig. 12 shows, only the long wavelength part of this band (notably the P_{13} branch, and the Q_{13},P_{23} band head[59]) has proved amenable to spectral simulation: At shorter wavelengths the congestion from overlapping branches, the probable involvement of the (1–2) band, and the indeterminate and, in all likelihood, wavelength dependent rotational state population distribution within the nascent CS(a) photofragments makes a complete band contour simulation impossible. Nonetheless, the breadth of the 1+1 REMPI bands implies that the CS($a\ ^3\Pi$) fragments are formed rotationally excited (our crude assignment assumes a rotational temperature of 2000 K), while our observation of the (0–2) band at an excitation wavelength where CS($a\ ^3\Pi)_{v=2}$ fragments are only just energetically allowed (by a two photon dissociation of CS_2) suggests that the dissociation dynamics also favor energy disposal into product vibration.

REMPI signals attributable to ground state C atoms arising in the multiphoton dissociation and/or ionization of CS_2 were observed at excitation wavelengths ca. 287 and 280 nm (2+1 REMPI) and ca. 395 nm (3+1 REMPI). As Fig. 13 shows, the former exhibit the full multiplet structure expected[46,61] of the $^3D_J\leftarrow{}^3P_J$ and $^3P_J\leftarrow{}^3P_J$ two photon resonances associated with the electron promotion $2p^13p^1\leftarrow2p^2$. Further discussion of these various atomic resonances and observed S atomic resonances is probably unwarranted given our lack of knowledge about the various C and S atom production mechanisms.

CONCLUSIONS

This study of the Rydberg state spectroscopy of the CS_2 molecule in the energy range 56 000–81 000 cm^{-1} provides further illustration of the wealth of detailed information that can be gleaned from careful studies involving the REMPI technique, especially when combined with parallel measurements of the kinetic energies of the resulting photoelectrons. The present study affords

(i) the most complete explanation yet available for the pattern of tangled spin–orbit split vibronic structure associ-

ated with the $^3\Pi_u$ and $^1\Pi_u$ states derived from the configuration $[^2\Pi_g]4p\sigma_u$ and the $^3\Delta_u$, $^1\Delta_u$, and $^1\Sigma_u^+$ states resulting from the configuration $[^2\Pi_g]4p\pi_u$, and allows estimation of an approximate wave number for the origin of the hitherto unidentified $^3\Sigma_u^+$ state derived from this same $[^2\Pi_g]4p\pi_u$ configuration;

(ii) determination of the origins of the next ($n=5$) members of four of these $[^2\Pi_g]np$ Rydberg series;

(iii) identification of extensive series based on the Rydberg configurations $[^2\Pi_g]ns\sigma_g$ and $[^2\Pi_g]nf\lambda_u$ with, in both cases, $n\leqslant 10$.

We also identify MPI resonances attributable to CS($a\ ^3\Pi$) fragments, to ground state C atoms, and to S atoms in both their ground (^3P) and excited (^1S) electronic states. Analysis of the former resonances indicates that the CS($a\ ^3\Pi$) fragments resulting from two photon dissociation of CS_2 at excitation wavelengths ca. 300 nm are formed with substantial rovibrational excitation.

ACKNOWLEDGMENTS

Financial support of the Bristol group from the EPSRC (previously SERC) in the form of equipment grants and a studentship (to R.A.M.) is gratefully acknowledged, as is the unstinting practical help and encouragement of Mr. K. N. Rosser. A.J.O.-E. is grateful to the Royal Society for the award of the Eliz. Challenor Research Fellowship and M.N.R.A. is grateful to the Ciba Fellowship Trust for their support of the Bristol–Amsterdam collaboration. The Amsterdam group is happy to acknowledge the Netherlands Organization for Scientific Research (N.W.O.) for equipment grants and financial support.

[1] W. C. Price and D. M. Simpson, Proc. R. Soc., London, Ser. A **165**, 272 (1938).
[2] B. Kleman, Can. J. Phys. **41**, 357 (1963).
[3] A. E. Douglas and I. Zanon, Can. J. Phys. **42**, 627 (1964).
[4] G. Herzberg, *Molecular Spectra and Molecular Structure, Vol. III. Electronic Spectra and Electronic Structure of Polyatomic Molecules* (van Nostrand Reinhold, Princeton, 1966).
[5] J. W. Rabalais, J. M. McDonald, V. Scherr, and S. P. McGlynn, Chem. Rev. **71**, 73 (1971), and references therein.
[6] Ch. Jungen, D. N. Malm, and A. J. Merer, Chem. Phys. Lett. **16**, 302 (1972).
[7] Ch. Jungen, D. N. Malm, and A. J. Merer, Can. J. Phys. **51**, 1471 (1973).
[8] F. R. Greening and G. W. King, J. Mol. Spectrosc. **59**, 312 (1976).
[9] M. N. R. Ashfold, M. T. Macpherson, and J. P. Simons, Topics Curr. Chem. **86**, 1 (1979), and references therein.
[10] D. G. Wilden and J. Comer, Chem. Phys. **53**, 77 (1980).
[11] M.-J. Hubin-Franskin, J. Delwiche, A. Poulin, B. Leclerc, P. Roy, and D. Roy, J. Chem. Phys. **78**, 1200 (1983), and references therein.
[12] A. J. Merer, S. A. Morris, and Ch. Jungen, J. Mol. Spectrosc. **127**, 425 (1988).
[13] R. McDiarmid and J. P. Doering, J. Chem. Phys. **91**, 2010 (1989).
[14] K. O. Lantz, V. Vaida, and D. J. Donaldson, Chem. Phys. Lett. **184**, 152 (1991).
[15] R. Mualem and A. Gedanken, Chem. Phys. Lett. **188**, 383 (1992).
[16] H. Bitto, A. Ruzicic, and J. R. Huber, Chem. Phys. **189**, 713 (1994), and references therein.
[17] S. V. Filseth, Adv. Photochem. **10**, 1 (1977), and references therein.
[18] G. Black, R. L. Sharpless, and T. G. Slanger, J. Chem. Phys. **66**, 2113 (1977).
[19] M. N. R. Ashfold, A. M. Quinton, and J. P. Simons, J. Chem. Soc. Faraday 2 **76**, 905, 915 (1980).
[20] S. C. Yang, A. Freedman, M. Kawasaki, and R. Bersohn, J. Chem. Phys. **72**, 4058 (1980).
[21] M. C. Addison, R. J. Donovan, and C. Fotakis, Chem. Phys. Lett. **74**, 58 (1980).
[22] J. E. Butler, W. S. Drozdoski, and J. R. McDonald, Chem. Phys. **50**, 413 (1980).
[23] G. Dornhöfer, W. Hack, and W. Langel, J. Phys. Chem. **88**, 3060 (1984).
[24] V. R. McCrary, R. Lu, D. Zakheim, J. A. Russell, J. B. Halpern, and W. M. Jackson, J. Chem. Phys. **83**, 3481 (1985).
[25] G. Black and L. E. Jusinski, Chem. Phys. Lett. **124**, 90 (1986).
[26] H. Kanamori and E. Hirota, J. Chem. Phys. **86**, 3901 (1987).
[27] I. M. Waller and J. W. Hepburn, J. Chem. Phys. **87**, 3261 (1987).
[28] W.-B. Tzeng, H.-M. Yin, W.-Y. Leung, J.-Y. Luo, S. Nourbakhsh, G. D. Flesch, and C. Y. Ng, J. Chem. Phys. **88**, 1658 (1988).
[29] S. P. Sapers and D. J. Donaldson, J. Phys. Chem. **94**, 8918 (1990); Chem. Phys. Lett. **198**, 341 (1992).
[30] C. Starrs, M. N. Jego, A. Mank, and J. W. Hepburn, J. Phys. Chem. **96**, 6526 (1992).
[31] I. Reineck, B. Wanneberg, H. Veerhuizen, C. Nohre, R. Maripuu, K. E. Norell, L. Mattson, L. Karlsson, and K. Siegbahn, J. Electron. Spectrosc. **34**, 235 (1984).
[32] M. Endoh, M. Tsuji, and Y. Nishimura, Chem. Phys. Lett. **109**, 35 (1984).
[33] L. S. Wang, J. E. Reutt, Y. T. Lee, and D. A. Shirley, J. Electron. Spectrosc. **47**, 167 (1988).
[34] I. Fischer, A. Lochschmidt, A. Strobel, G. Niedner-Schatteburg, K. Müller-Dethlefs, and V. E. Bondybey, Chem. Phys. Lett. **202**, 542 (1993).
[35] M. N. R. Ashfold and J. D. Howe, Ann. Rev. Phys. Chem. **45**, 57 (1994).
[36] S. Couris, E. Patsilinakou, M. Lotz, E. R. Grant, C. Fotakis, C. Cossart-Magos, and M. Horani, J. Chem. Phys. **100**, 3514 (1994).
[37] L. Li, X. T. Wang, X. N. Li, and X. B. Xie, Chem. Phys. **164**, 305 (1992).
[38] L. Li, X. T. Wang, X. N. Li, and X. B. Xie, Chem. Phys. Lett. **202**, 115 (1993).
[39] J. Baker, M. Konstantaki, and S. Couris, J. Chem. Phys. **103**, 2436 (1995).
[40] J. Baker and S. Couris, J. Chem. Phys. **103**, 4847 (1995).
[41] C. Cossart-Magos, M. Jungen, and F. Launay, Mol. Phys. **61**, 1077 (1987).
[42] M. Wu and P. M. Johnson, J. Chem. Phys. **91**, 7399 (1989).
[43] P. Johnson and M. Wu, J. Chem. Phys. **94**, 868 (1991).
[44] M. Wu, D. P. Taylor, and P. M. Johnson, J. Chem. Phys. **94**, 7596 (1991); *ibid.* **95**, 761 (1991).
[45] D. P. Taylor and P. M. Johnson, J. Chem. Phys. **98**, 1810 (1991).
[46] M. R. Dobber, W. J. Buma, and C. A. de Lange, J. Chem. Phys. **101**, 9303 (1994).
[47] C. Cossart-Magos, H. Lefebvre-Brion, and M. Jungen, Mol. Phys. **85**, 821 (1995).
[48] B. Yang, M. H. Eslami, and S. L. Anderson, J. Chem. Phys. **89**, 5527 (1988).
[49] R. Weinkauf and U. Boesl, J. Chem. Phys. **98**, 4459 (1993).
[50] R. A. Morgan, A. J. Orr-Ewing, D. Ascenzi, M. N. R. Ashfold, W. J. Buma, C. R. Scheper, and C. A. de Lange (unpublished).
[51] M. N. R. Ashfold, W. S. Hartree, A. V. Salvato, B. Tutcher, and A. Walker, J. Chem. Soc. Faraday Trans. **86**, 2027 (1990).
[52] M. N. R. Ashfold, A. D. Couch, R. N. Dixon, and B. Tutcher, J. Phys. Chem. **92**, 5327 (1988).
[53] B. G. Koenders, D. M. Wieringa, K. E. Drabe, and C. A. de Lange, Chem. Phys. **118**, 13 (1987).
[54] N. P. L. Wales, E. de Beer, N. P. C. Westwood, W. J. Buma, C. A. de Lange, and M. C. van Hemert, J. Chem. Phys. **100**, 7984 (1994).
[55] W. C. Martin, R. Zalubas, and A. Musgrove, J. Phys. Chem. Ref. Data **19**, 821 (1990).
[56] S. Woutersen, J. B. Milan, W. J. Buma, and C. A. de Lange (unpublished).
[57] H. Lefebvre-Brion and R. W. Field, *Perturbations in the Spectra of Diatomic Molecules* (Academic, New York, 1986).
[58] A. Gedanken, J. Phys. Chem. **92**, 5862 (1988).
[59] Y. Ono and J. L. Hardwick, J. Mol. Spectrosc. **119**, 107 (1986).
[60] K. P. Huber and G. Herzberg, *Molecular Spectra and Molecular Structure IV: Constants of Diatomic Molecules* (van Nostrand Reinhold, New York, 1979).
[61] S. Bashkin and J. O. Stoner, Jr., *Atomic Energy Levels and Grotrian Diagrams* (North Holland, Amsterdam, 1975), Vol. 1.